Encapsulation of lipophilic kiteplatin Pt(IV) prodrugs in PLGA-PEG micelles.

Nicola Margiotta,[1,*] *Salvatore Savino,*[1] *Nunzio Denora,*[2] *Cristina Marzano,*[3] *Valentino Laquintana,*[2] *Annalisa Cutrignelli,*[2] *James D. Hoeschele,*[4] *Valentina Gandin,*[3] *Giovanni Natile.*[1,*]

[1]Dipartimento di Chimica, Università degli Studi di Bari Aldo Moro, via E. Orabona 4, 70125 Bari (Italy);

[2]Dipartimento di Farmacia-Scienze del Farmaco, Università degli Studi di Bari Aldo Moro, via E. Orabona 4, 70125 Bari (Italy);

[3]Dipartimento di Scienze del Farmaco, Università di Padova, via Marzolo 5, 35131 Padova (Italy);

[4]Department of Chemistry, Eastern Michigan University, Ypsilanti, MI, USA 48197.

***Corresponding Authors**

Phone: +39 080 5442759 (N.M.); +39 080 5442774 (G.N.). E-mail: nicola.margiotta@uniba.it (N.M.); giovanni.natile@uniba.it (G.N.).

Abstract

Biodegradable, PEG-coated, nanoparticles (NPs) have gained therapeutic application as injectable colloidal systems for the controlled and site-specific release of drugs. In this paper, encapsulation in PLGA-PEG polymer NPs has been exploited to lower toxicity and increase the antitumor activity of kiteplatin ([$PtCl_2$(*cis*-1,4-DACH)]). Kiteplatin contains an isomeric form of the diamine ligand present in oxaliplatin and proved to be particularly active against ovarian and colon cancers. To favor encapsulation of the platinum drug in the hydrophobic core of the polymeric micelles, Pt(IV) prodrugs having hydrophobic carboxylic ligands at the axial positions were used in place of hydrophilic Pt(II) complexes (compounds **1**-**4**). The size, size distribution, and zeta potential (ZP) were measured by dynamic light scattering (DLS) and laser Doppler velocimetry (LDV), and the

drug encapsulation efficiency (EE) correlated to the alkyl chain length of the different Pt(IV) prodrugs. The number of the Pt atoms per NP (in the range of 1.3-2.4 $\cdot 10^6$) is comparable to that of polysilsesquioxane-based NP and higher than that found for other nanoparticle platforms. The platinum-loaded PLGA-PEG NPs, tested *in vivo* in a syngeneic murine solid tumor (LLC), had higher antitumor effect and, most importantly, were markedly less toxic than kiteplatin.

Introduction

Cisplatin (Chart 1) is one of the most widely used chemotherapeutic agents for the treatment of testicular, ovarian, bladder, and lung cancers, melanoma, lymphomas, and myelomas.[1]

The clinical efficacy demonstrated by platinum-based drugs currently approved by the FDA (Chart 1) has prompted an intense research aiming to discover new metal-based drugs with enhanced efficacy, lower toxicity, and a broader spectrum of activity.[2]

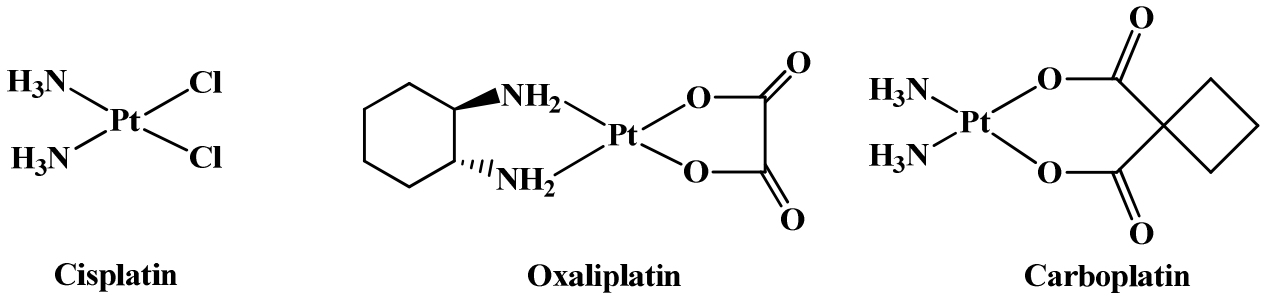

Cisplatin **Oxaliplatin** **Carboplatin**

Chart 1. Platinum drugs currently approved by FDA.

Several advantages can be obtained by the use of nanosized drug delivery vehicles.[3] The controlled release provided by these systems can enhance retention in the bloodstream, their size allows for passive targeting, and their surfaces can be functionalized for active targeting. Targeted and controlled drug delivery can improve dramatically the degree and duration of the clinical outcome.

Therefore, in the last decades the use of biodegradable nanoparticles (NPs) for drug delivery has increased steeply.[4,5,6,7,8] Nanosystems for the delivery of metallodrugs have been extensively reviewed in the last decade.[9,10,11,12,13]

The NPs size can be modified to obtain organ specific biodistribution,[14] such as in the case of splenic sequestration of liposomes that decreases linearly with decrease in particle size.[15,16] Unlike spleen, the sequestration by liver has non-linear dependence on size and both large and small NPs are sequestered. Small NPs can pass through the sinusoidal fenestrations present in the liver and be entrapped by underlying parenchymal cells.[17] Therefore, the effect of NPs size differs from organ to organ, underscoring the importance of tuning NPs size for each distinct application.

Conventional colloidal drug delivery systems, such as liposomes, are rapidly cleared from the systemic circulation, and they end almost exclusively in the mononuclear phagocyte system,[18] this type of uptake can be advantageous for the treatment of illness of the reticuloendothelial system (RES) because it provides high local concentration of therapeutic agent.[19] For delivering a drug to sites other than RES, stealth liposomes appear to be more suitable. Indeed, stealth nanoparticles decorated on their surface with poly(ethylene glycol) (PEG) are characterized by long circulating time.[20,21,22,23]

Thus, biodegradable, PEG-coated, NPs have gained therapeutic application as injectable colloidal systems for the controlled and site-specific release of drugs.[24,25,26] If compared to other long-circulating systems, stealth NPs show better shelf stability and greater ability to control the release of the encapsulated compounds.[20,25] Tobio et al. studied PEGylated polylactic acid albumin (PEG–PLA) NPs as tetanus toxoid carriers for nasal administration.[21] Recently, PEGylated poly(lactic-co-glycolic acid) (PEG–PLGA) NPs have been used as carriers for both hydrophobic and hydrophilic drugs.[20,27]

Lippard and collaborators reported a strategy for delivering the platinum(IV) compound *cis,trans,cis*-$[PtCl_2\{O_2C(CH_2)_4CH_3\}_2(NH_3)_2]$ to prostate cancer cells. The drug was loaded on PLGA-*b*-PEG NPs carrying on their surface aptamers (Apt)[28,29] targeting the Prostate Specific Membrane Antigen (PSMA).[30,31,32] In order to favor encapsulation of the platinum drug in the hydrophobic core of the polymeric micelles, Pt(IV)-prodrugs having hydrophobic carboxylate

ligands at the axial positions were used in place of hydrophilic Pt(II) complexes. A lethal dose of platinum(II) drug is delivered upon intracellular reduction of the Pt(IV) prodrug.[33,34,35,36]

The chemical properties of the carboxylate ligands can be correlated with the efficiency of encapsulation in nanoparticles. In particular, as the chain length increases, also the level of platinum(IV) encapsulation increases.[37]

A series of Pt(IV) prodrugs derived from [$PtCl_2$(*cis*-1,4-DACH)] (Kiteplatin, DACH = diaminocyclohexane), by addition of two carboxylate ligands (with different length of the alkyl chains) in axial positions, was already synthesized and tested for antitumor activity in the murine L1210/0 leukemia model by Khokhar et al.[38] Kiteplatin contains an isomeric form of the diamine ligand present in oxaliplatin and proved to be particularly active against cell lines sensitive and resistant to cisplatin (2008/C13* ovarian cancer cells) and oxaliplatin (LoVo/LoVo-OXP colon cancer cells).[39] Because of its unique properties, kiteplatin has been extensively investigated also in recent years with emphasis on its reactivity and mechanism of action.[40,41,42,43,44,45,46] In the present paper we have investigated the encapsulation in PLGA-PEG polymer nanoparticles of four Pt(IV) prodrugs reported by Khokhar differing for lipophilicity: *cis,trans,cis*-[$PtCl_2\{O_2C(CH_2)_nCH_3\}_2$(*cis*-1,4-DACH)] (n = 4, 8, 0, 2 corresponding, respectively, to compounds **1**, **2**, **3**, and **4** in Chart 2; we assigned number **1** and **2** to the most extensively investigated compounds of the series). The aim was that of exploiting targeting and increase of circulating time typical of NPs for lowering the toxicity and increase the antitumor activity of kiteplatin. In Scheme 1 is shown the self-assembling of polymer and Pt(IV) drug in micelles in which the hydrophobic platinum substrate concentrates in the core.

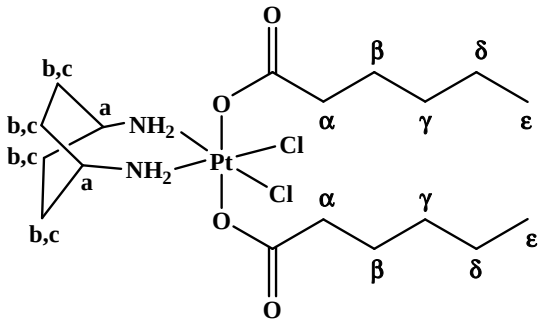

cis,trans,cis[$PtCl_2\{O_2C(CH_2)_4CH_3\}_2$(*cis*-1,4-DACH)] (1)

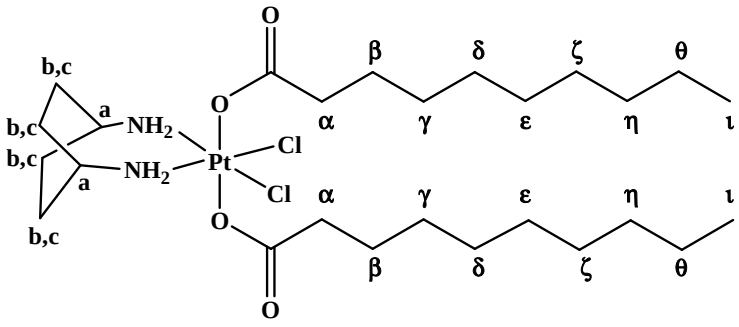

cis,trans,cis[$PtCl_2\{O_2C(CH_2)_8CH_3\}_2$(*cis*-1,4-DACH)] (2)

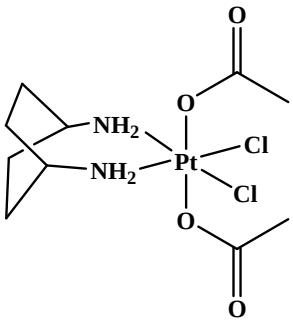

cis,trans,cis[$PtCl_2(O_2CCH_3)_2$(*cis*-1,4-DACH)] (3)

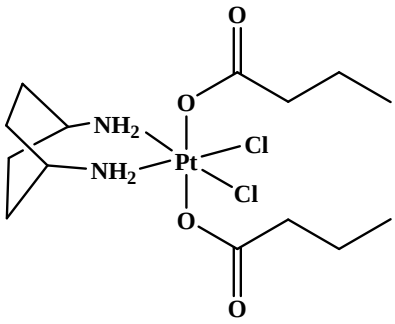

cis,trans,cis[$PtCl_2\{O_2C(CH_2)_2CH_3\}_2$(*cis*-1,4-DACH)] (4)

Chart 2. Pt(IV) prodrugs of kiteplatin having in the axial positions *trans*-carboxylate ligands with different alkyl chains.

The size, size distribution, and zeta potential (ZP) of **1**-PLGA-PEG, **2**-PLGA-PEG, **3**-PLGA-PEG and **4**-PLGA-PEG were measured by dynamic light scattering (DLS) and Laser Doppler Velocimetry (LDV), respectively. Furthermore, the drug encapsulation efficiency (EE) was correlated to the alkyl chain length of the different Pt(IV) prodrugs.

Finally, the antitumor activity of compounds **1** and **2** loaded in PLGA-PEG nanoparticles was evaluated in a syngeneic murine solid tumor model, the Lewis Lung Carcinoma (LLC).

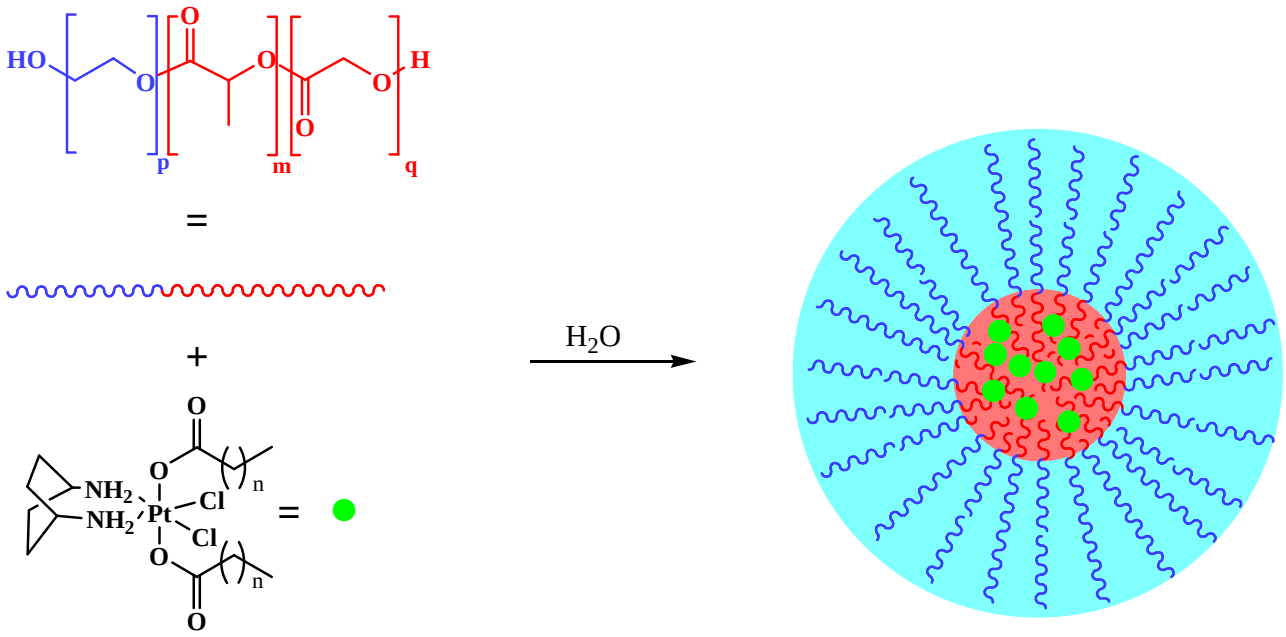

Scheme 1. Schematic representation of the nanoprecipitation process, whereby the amphiphilic block copolymer chains self-assemble into micelles trapping the hydrophobic platinum drugs in the core.

Experimental

Materials and methods

Commercial reagent grade chemicals and solvents were used as received without further purification. ^{1}H-NMR, COSY and TOCSY 2D NMR spectra were recorded on a Bruker Avance III 700 MHz instrument. The Fourier transform infrared spectrum of the PLGA-PEG copolymer was recorded on a Perkin Elmer Spectrum One instrument. [^{1}H-^{13}C]-HSQC spectra were recorded on Bruker Avance DPX 300 MHz and Bruker Avance III 700 MHz instruments. ^{1}H and ^{13}C chemical shifts were referenced using the internal residual peak of the solvent (DMSO-d_6: 2.50 ppm for ^{1}H and 39.51 ppm for ^{13}C). [^{1}H-^{195}Pt] HSQC spectra were recorded on Bruker Avance DPX 300 MHz instrument. ^{195}Pt NMR spectra were referenced to K_2PtCl_4 (external standard placed at −1620 ppm with respect to $Na_2[PtCl_6]$).[47]

Electrospray ionisation mass spectrometry (ESI-MS) was performed with an electrospray interface and an ion trap mass spectrometer (1100 Series LC/MSD Trap system Agilent, Palo Alto, CA). Elemental analyses were carried out with an Eurovector EA 3000 CHN instrument.

Kiteplatin,[39] *cis,trans,cis*-[$PtCl_2(OH)_2$(*cis*-1,4-DACH)],[46] *cis,trans,cis*-[$PtCl_2(O_2CCH_3)_2$(*cis*-1,4-DACH)] (**3**),[38] and *cis,trans,cis*-[$PtCl_2\{O_2C(CH_2)_2CH_3\}_2$(*cis*-1,4-DACH)] (**4**)[38] were prepared according to already reported procedures and all analytical data were in good agreement with the given formulation (data not shown).

Synthesis of *cis,trans,cis*-[$PtCl_2\{O_2C(CH_2)_4CH_3\}_2$(*cis*-1,4-DACH)] (1). This compound was prepared according to a procedure reported in the literature[38] with slight modifications. To a suspension of *cis,trans,cis*-[$PtCl_2(OH)_2$(*cis*-1,4-DACH)] (120 mg; 0.29 mmol) in 24 mL of acetonitrile, was added 1 mL of hexanoic anhydride (15-fold excess). The reaction mixture was refluxed at 80 °C for 15 h in the dark. The suspension was filtered and the filtrate was evaporated to dryness under reduced pressure. The resulting yellow residue was redissolved in acetone and the subsequent addition of n-pentane led to the precipitation of a pale brown solid that was isolated by filtration, washed with water, and dried under vacuum. Yield 57% (101 mg, 0.165 mmol).

Anal.: calculated for $C_{18}H_{36}Cl_2N_2O_4Pt\cdot\frac{1}{2}H_2O$ (**1**$\cdot\frac{1}{2}H_2O$): C, 34.90; H, 6.02; N, 4.52 %. *Found*: C, 34.72; H, 5.70; N, 5.17 %. ESI-MS in MeOH: *calculated for* $C_{18}H_{36}Cl_2N_2O_4PtNa$, [**1** + Na]$^+$ 633.15. *Found:* $^m/_z$ 633.17. ^{1}H NMR (DMSO-d_6): 8.18 (4H, NH_2), 2.96 (2H, CHa), 2.22 (4H, CHα), 1.58 (8H, CHb,c), 1.47 (4H, CHβ), 1.24 (8H, CHγ,δ), 0.84 (6H, CHε) ppm (see Chart 2 for numbering of protons). ^{195}Pt NMR (DMSO-d_6): 1215.9 ppm. ^{13}C NMR (DMSO-d_6): 13.67, 19.73, 21.64, 24.8, 30.42, 36.03, and 49.34 ppm.

Synthesis of *cis,trans,cis*-[$PtCl_2\{O_2C(CH_2)_8CH_3\}_2$(*cis*-1,4-DACH)] (2). This compound was prepared as described for complex **1** with some differences in the purification step. To a suspension of *cis,trans,cis*-[$PtCl_2(OH)_2$(*cis*-1,4-DACH)] (84.6 mg; 0.20 mmol) in 17 mL of acetonitrile, was

added 1.0 g of decanoic anhydride (15-fold excess). The reaction mixture was refluxed at 80 °C for 15 h in the dark and then cooled to room temperature meanwhile a white crystalline compound separated. The crystals were isolated by filtration of the mother liquor, washed with diethyl ether and dried under vacuum. Yield 59% (85.3 mg, 0.118 mmol). *Anal.: calculated for* $C_{26}H_{52}Cl_2N_2O_4Pt \cdot H_2O$ (**2**·H_2O): C, 42.16; H, 7.35; N, 3.78 %. *Found*: C, 41.69; H, 7.01; N, 3.68 %. ESI-MS in MeOH: *calculated for* $C_{26}H_{51}Cl_2N_2O_4Pt$, [**2** - H]$^-$ 721.28. *Found :* $^m/_z$ 721.30. ^{1}H NMR (DMSO-d_6): 8.19 (4H, NH_2), 2.96 (2H, CHa), 2.23 (4H, CHα), 1.59 (8H, CHb,c), 1.48 (4H, CHβ), 1.23 (24H, CHγ,δ,ε,ζ,η,θ), 0.85 (6H, CHι) ppm (see Chart 2 for numbering of protons). ^{195}Pt NMR (DMSO-d_6): 1217.2 ppm. ^{13}C NMR (DMSO-d_6): 13.7, 19.77, 21.7, 25.22, 28.54, 30.97, 36.27, 49.40 ppm.

Synthesis of PLGA-PEG. The carboxy-terminated amphiphilic poly(D,L-lactide–*co*–glycolic acid)-block-poly(ethylene glycol) (PLGA-PEG) copolymer was prepared by conjugation of PEG4000 (PEG) to non-end-capped poly(D,L-lactide–*co*–glycolide) (50/50) with hydroxyl and carboxylate terminal groups (PLGA; RG503H, Mw 34 kDa, Boehringer Ingelheim, Germany) according to a procedure reported in the literature with minor modifications.[48] Briefly, PLGA (1 g, 0.03 mmol) in anhydrous THF (15 mL) was converted to PLGA–OBt with excess 1-Hydroxybenzotriazole (HOBt, 40 mg, 0.30 mmol) in the presence of *N*,*N*′-dicyclohexylcarbodiimide (DCC, 61 mg, 0.30 mmol). After 30 minutes, a solution of PEG (0.118 g, 0.03 mmol) in anhydrous DMF (15 mL) was added to the PLGA-OBt reaction mixture and stirring was protracted overnight. The reaction mixture was cooled to 0 °C and the resulting precipitate, dicyclohexylurea, was removed by filtration. The filtrate, after drying under vacuum, was dissolved in methylene chloride (5 mL) and treated with cold ethyl ether (50 mL) to precipitate the PLGA-PEG copolymer. The copolymer was washed with diethyl ether (3 x 10 mL) to remove excess of unreacted reagents. The resulting PLGA–PEG block *co*-polymer was dried under vacuum and used for NPs preparation without further treatment. Obtained 1.03 g (65 % yield). FT-IR (KBr): 3504,

1760, 1172-1062 cm^{-1}. ^1H NMR ($CDCl_3$): 1.59 (m, $[–C(O)CH(CH_{3a})O–]_m$), 3.64 (s, $[–CH_{2b}CH_{2b}O–]_p$), 4.84 (m, $[–C(O)CH_{2c}–]_q$), 5.22 (m, $[–C(O)CH_d(CH_3)O–]_m$) ppm (see Figure 1 for numbering of protons).

Preparation of drug loaded PLGA-PEG NPs.[37] A DMF solution (550 μL) was prepared by mixing 10 mg of PLGA-PEG and 1 mg of the platinum complex (**1**, **2**, **3**, or **4**) so to have a 10% of Pt feed, defined as (mg of Pt complex/mg of polymer) × 100. An aliquot of this solution (500 μL) was added dropwise, over 10 min time, to 5 mL of fastly stirred Milli-Q water. After addition of the DMF solution, water acquired a milky blue coloration owing to Tyndall scattering of the formed nanoparticles. An aqueous solution of poly(vinyl alcohol) (5 mL, 0.1% w/w PVA) was then added along the edge of the vial so to bring the final volume to 10.5 mL and the final PVA concentration to approximately 0.05% w/w. This suspension of NPs was stirred for additional 20 min and then passed through a 0.45 μm cellulose acetate syringe filter (VWR). The filtrate was loaded into an Amicon Centrifugal Filtration Device (3 kDa MWCO regenerated cellulose (R.G.) membrane). The loaded device was centrifuged at 6000g for 20 min, concentrating the nanoparticle suspension to approximately 1 mL. This concentrated material was suspended in 10 mL of fresh Milli-Q water and centrifuged again under identical conditions. The latter operation was repeated two more times. All nanoprecipitations were carried out in triplicate.

Size Exclusion Chromatography (SEC).

Average molecular weights and molecular weight distributions of the PLGA-PEG copolymer were obtained by SEC, using a Waters Associates (Milford, MA) Model 1515 HPLC isocratic pump, a differential RID detector Waters 2414 and a UltraHydrogel TM 500 column (7.8 x 300 mm, 5μm). Water was used as mobile phase, at 30 °C, with a flow rate of 0.6 mL/min. Calibration was performed using a series of polyethylene glycol/oxide (PEG/PEO) standards (Agilent technologies). Chromatographic data were processed by Waters Associates (Milford, Ma) Breeze software.

Evaluation of PLGA-PEG NPs Encapsulation. To evaluate the encapsulation efficacy we measured the platinum present in 100 μL of the colloidal suspension. This suspension was digested with 2 mL of HNO_3 (67%)/H_2O_2 (30%), 1:1 (v/v), solution for 4 h at 60 °C. The platinum content was quantified by inductively coupled plasma mass spectrometry (ICP-MS). All ICP-MS measurements were carried out in triplicate and averaged.

Particle Size, Size Distribution and Surface Charge of drug loaded PLGA-PEG NPs. The average hydrodynamic diameters (*z*-average), size distribution (polydispersity index, DLS PDI) and zeta potential (ZP) of drug loaded PLGA-PEG NPs were detected using a Zetasizer Nano ZS, Malvern Instruments Ltd., Worcestershire, UK. The hydrodynamic diameters and size distribuition of the NPs were measured by dynamic light scattering (DLS) after suspension in demineralized water at a concentration of 0.1 mg NPs/mL. The ZP was determined by laser doppler velocimetry (LDV) after dilution of the samples with KCl 1 mM at a concentration of 0.05 mg NPs/mL.

Transmission Electron Microscopy Characterization (TEM). A JEOL med. 100 electron microscope operating at 100 kV equipped with a CCD high resolution camera was used for TEM analysis. Samples were prepared by dipping the carbon coated copper grid into a dilute solution of the PLGA-PEG NPs containing compounds **1** and **2** at the maximum feed and let the solvent to evaporate.

***In Vivo* Anticancer Activity toward Lewis Lung Carcinoma (LLC).** All studies involving animal testing were carried out in accordance with the ethical guidelines for animal research adopted by the University of Padua, acknowledging the Italian regulation and European Directive 2010/63/UE as to the animal welfare and protection and the related codes of practice. The mice were purchased from Charles River, Italy, housed in steel cages under controlled environmental conditions (constant

temperature, humidity, and 12 h dark/light cycle), and alimented with commercial standard feed and tap water ad libitum. The LLC cell line was purchased from ECACC, United Kingdom. The LLC cell line was maintained in DMEM (Euroclone) supplemented with 10% heat inactivated fetal bovine serum (Euroclone), 10 mM L-glutamine, 100 U mL^{-1} penicillin, and 100 $\mu g \cdot mL^{-1}$ streptomycin in a 5% CO_2 air incubator at 37 °C. The LLC was implanted intramuscularly (i.m.) as a 2×10^6 cell inoculum into the right flank of 8 week old male and female C57BL mice (24 ± 3 g body weight). After 7 days from tumor implantation (visible tumor), mice were randomly divided into 6 groups (5 animals per group) and subjected to daily *i.p.* administration of PLGA-PEG nanoparticles loaded with 1.7 mg kg^{-1} of **1** or **2**, kiteplatin (1.7 mg kg^{-1} in saline solution), cisplatin (1.7 mg kg^{-1} in saline solution), unloaded PLGA-PEG nanoparticles or the vehicle solution (saline solution). At day 15, animals were sacrificed, the legs were amputated at the proximal end of the femur, and the inhibition of tumor growth was determined according to the difference in weight of the tumor-bearing leg and the healthy leg of the animals expressed as a percentage referring to the control animals. Body weight was measured every 2 days and was taken as a parameter for systemic toxicity. All reported values are the means ± SD of no less than three measurements. Multiple comparisons were made by the Tukey−Kramer test (**, $p < 0.01$; * or °, $p < 0.05$).

Results and Discussion

Unlike kiteplatin, whose hydrophilicity ($logP_{o/w} = -1.57 \pm 0.10$)[39] renders the compound unsuitable for encapsulation in nanoparticles, the Pt(IV) counterpart, obtained by addition of axial ligands with high lipophilicity, are suitable for encapsulation in the hydrophobic core of micelles. Therefore, a series of Pt(IV) derivatives of kiteplatin was prepared, having in axial position the ligands acetate (**3**), butanoate (**4**), hexanoate (**1**), and decanoate (**2**).

All four Pt(IV) derivatives were prepared by a similar synthetic approach based on the oxidation of kiteplatin to the corresponding Pt(IV) dihydroxido derivative by hydrogen peroxide in water

followed by condensation with the corresponding carboxylic anhydride (refluxing for 15 h in acetonitrile) to yield the dicarboxylato complexes (Scheme 2).[38,49,50,51]

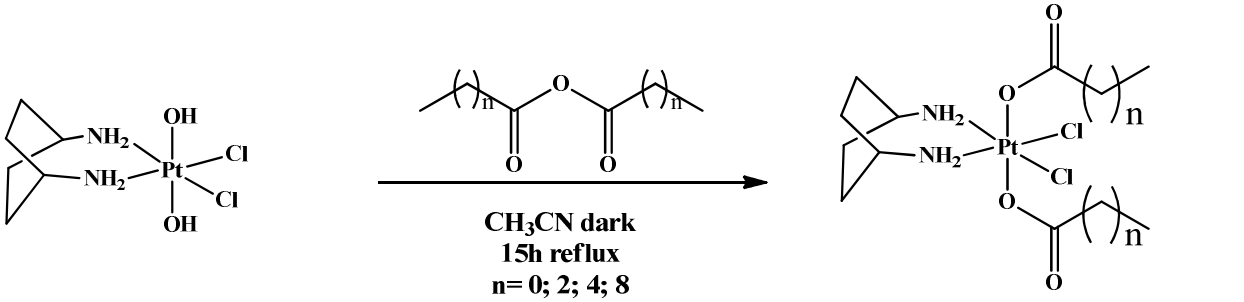

***cis,trans,cis*-[$PtCl_2(OH)_2$(*cis*-1,4-DACH)]** **1 (n = 4); 2 (n = 8); 3 (n = 0); 4 (n = 2)**

Scheme 2. Synthesis of the lipophilic Pt(IV) dicarboxylato species.

All compounds were characterized by elemental analysis, ESI-MS, and NMR. The ESI-MS spectrum of compound **1** showed the presence of a peak at *m/z* = 633.15 corresponding to $[\mathbf{1}+Na]^+$ and the experimental isotopic pattern of the peak was in good agreement with the theoretical one (data not shown). The ^1H NMR spectrum in DMSO-d_6 showed seven different signals (Figure S1 in Supporting Information). The singlet with Pt satellites falling at 8.18 ppm ($^2J_{H\text{-}Pt}$ = 61.09 Hz) was assigned to the aminic protons of coordinated *cis*-1,4-DACH. The singlet with Pt satellites resonating at 2.96 ppm ($^3J_{Pt\text{-}H}$ = 80 Hz) was assigned to the methynic protons of coordinated DACH while the multiplet integrating for eight protons and located at 1.58 ppm was assigned to the methylenic protons of coordinated DACH. The triplet located at 2.22 ppm, and integrating for 4 protons, was assigned to the α CH_2 groups of coordinated hexanoates; the β CH_2 groups give a quintet resonating at 1.47 ppm, while the CH_2 groups in γ and δ positions (Chart 2) give the multiplet falling at 1.24 ppm and integrating for eight protons. Finally, the triplet resonating at 0.84 ppm and integrating for six protons was attributed to the terminal methyl groups of the alkyl chains. This assignment was supported by a COSY 2D NMR spectrum recorded in DMSO-d_6. A portion of this spectrum is reported in Figure S2 in the Supplementary Information.

The [^1H-^{195}Pt]-HSQC 2D NMR spectrum (Figure S3 in Sup. Info) shows two cross peaks falling at 8.18/1215.9 and 2.96/1215.9 ppm ($^1H/^{195}Pt$). The ^{195}Pt chemical shift is in good agreement with

those reported in the literature for analogous lipophilic complexes, such as *cis,trans,cis*-$[PtCl_2\{O_2C(CH_2)_4CH_3\}_2(NH_3)_2]$ (1217.79 ppm in DMSO-d_6).[32] Khokhar reported for compound **1** a ^{195}Pt chemical shift of 1085 ppm but the solvent used was $CDCl_3$ instead of DMSO-d_6.

The NMR characterization of the carbon atoms was obtained by a [^1H-^{13}C]-HSQC 2D NMR experiment also performed in DMSO-d_6 (Figure S4, Sup. Info). The cross peaks falling at 2.96/49.34 and 1.58/19.73 ppm ($^1H/^{13}C$), were attributed to the methynic and methylenic groups of DACH, respectively. The ^{13}C chemical shifts of the alkyl chain of the hexanoato ligands (13.67, 21.64, 24.8 30.42, and 36.03) are in good agreement with those reported in literature by Lippard for *cis,trans,cis*-$[PtCl_2\{O_2C(CH_2)_4CH_3\}_2(NH_3)_2]$ (13.93, 22.0, 25.14, 30.87, and 35.65 ppm).[32]

Compound **2** was also characterized by elemental analysis, ESI-MS, and NMR. The ESI-MS spectrum showed the presence of a peak at *m/z* = 721.30 corresponding to $[M-H]^-$ and the experimental isotopic pattern of the peak was in good agreement with the theoretical one (data not shown).

The NMR characterization of compound **2** (similar to that already described for compound **1**) is reported in the Experimental Section and in the Supplementary Information.

Synthesis and characterization of PLGA–PEG copolymer.

The PLGA–PEG block copolymer was synthesized by direct conjugation of the carboxylic end group of PLGA with PEG in DMF/THF 1:1 (v/v) using *N*,*N*′-Dicyclohexylcarbodiimide (DCC) and 1-Hydroxybenzotriazole (HOBt) as coupling reagents (Scheme 3). The PLGA–PEG copolymer was purified by precipitation with satisfactory yield.

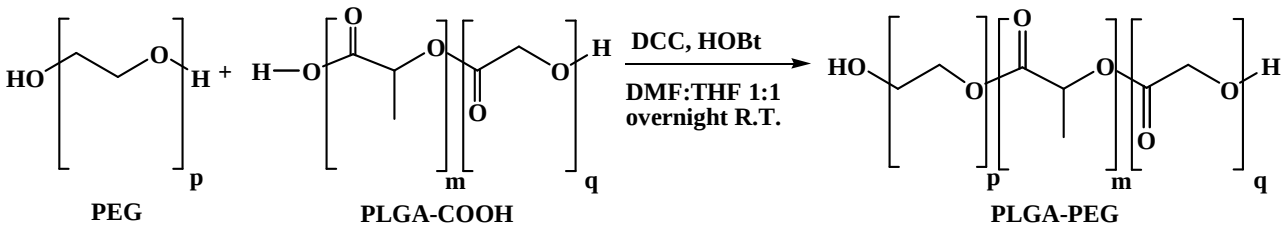

Scheme 3. Synthesis of PLGA–PEG.

^{1}H-NMR and FT-IR spectra are consistent with the given structure. The ^{1}H-NMR of PLGA-PEG copolymer is shown in Figure 1. The overlapping doublets integrating for three protons and falling at 1.59 ppm were attributed to the methyl groups of the lactic acid repeat units (a in Figure 1). The singlet falling at 3.64 ppm corresponds to the methylene groups of the PEG (b in Figure 1). The multiplets at 4.84 and 5.22 ppm were assigned to CH_2(c) of glycolic acid and CH(d) of lactic acid, respectively.

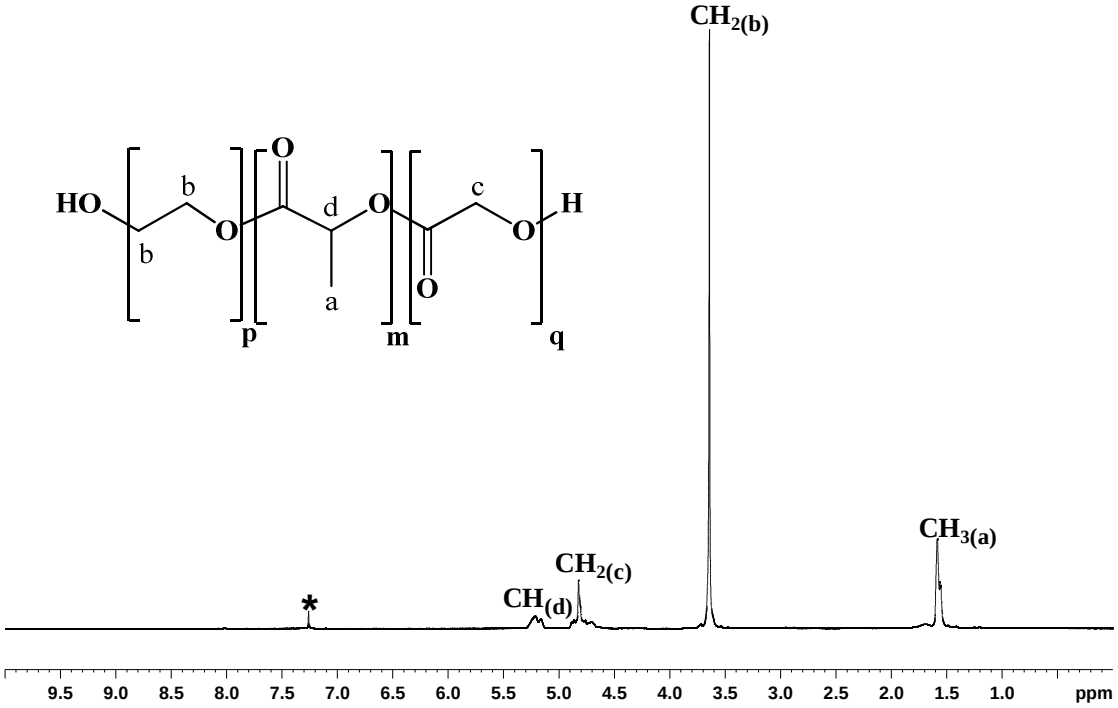

Figure 1. ^{1}H NMR (700 MHz, ^{1}H) spectrum of **PLGA-PEG** in $CDCl_3$. The asterisk indicates residual solvent peak.

The FT-IR spectrum (Figure S9) showed an absorption band at 3504 cm^{-1} corresponding to the terminal hydroxyl groups of PEG and glycolic acid. The strong band at 1760 cm^{-1} was assigned to the C=O stretching vibration, while the bands in the range 1172.4-1061.6 cm^{-1} are due to C-O stretching vibration.

Unlike small molecules, polymers have not a unique molecular weight but cover a range of molecular weights. The distribution will depend upon the synthetic procedure used. Hence, for the characterization of polymers must be considered both the distribution of molecular weights and the mean molecular weight M.

There are two different ways to estimate the average molecular weight: Number-Average Molecular Weight (M_n) and Weight-Average Molecular Weight (M_w).[52] M_n is relevant to properties which are only sensitive to the number of molecules present and are not influenced by the size of single particles in the mixture. Examples are the colligative properties of solutions such as boiling point elevation, freezing point depression, and osmotic pressure. This average molecular weight (M_n) is defined as the total weight of polymer divided by the number of polymer molecules.[52] M_w is relevant to properties which depend not only upon the number of polymer molecules but also upon their size or weight. A classic example is light scattering. M_w is defined by: $M_w = \frac{\sum_{i=1}^{\infty} N_i M_i^2}{\sum_{i=1}^{\infty} N_i M_i}$ where M_i is the molecular weight of a chain and N_i is the number of chains of that molecular weight. Compared to M_n, M_w takes into account the molecular weight of a chain in determining contributions to the molecular weight average. The more massive the chain, the more the chain contributes to M_w. Finally, M_p is used to indicate the molar mass corresponding to the peak maximum of the elugram of the polymer, it is a defined molar mass and not an average like M_n and M_w.

The spread of the distribution function can be characterized by its standard deviation or by its polydispersity index SEC PDI, that is the ratio between M_w and M_n (SEC PDI = M_w/M_n). For all real polymers SEC PDI is greater than one and the excess with respect to one is a measure of the

polydispersity of the polymer.[52] In the case of the polymer synthesized in this work, PLGA-PEG, the average molecular weights and M_p, determined by aqueous SEC, are in good agreement with a monodisperse system, and the SEC PDI (M_w/M_n) was 1.003, indicating a narrow range of molecular weights (Table 1).

Preparation and characterization of drug loaded PLGA–PEG NPs.

The poly(D,L-lactic acid-co-glycolic acid)-block-poly(ethyleneglycol) copolymer (PLGA-PEG) is biocompatible and biodegradable and its degradation process is well known.[53] Erosion studies on the degradation process of PLGA-PEG highlighted that ester hydrolysis and transesterification mechanisms are both responsible for the loss of copolymers mass. PLGA-PEG based NPs erosion starts with water uptake followed by random hydrolytic chain cleavage of the polyester block with release of oligomers.[54] The release of the hydrophobic drugs non-covalently loaded in PLGA-PEG NPs occurs quickly by passive diffusion through the intact matrix, whereas the release of drugs covalently bound to the backbone occurs more slowly and requires the participation of a hydrolytic process occurring simultaneously to or after the degradation of the matrix.[55]

The preparation of the Pt drug-loaded PLGA-PEG NPs was achieved by the nanoprecipitation method.[37] The PLGA-PEG copolymer and the platinum complex (mg polymer/mg Pt complex = 10) were dissolved in the water miscible solvent DMF, and then added dropwise into an aqueous solution, generating NPs. The NPs were characterized for their hydrodynamic size, size distribution and surface charge, the results are reported in Table 2.

The hydrodynamic size (average hydrodynamic diameter) of unloaded PLGA-PEG nanoparticles is 116.6 nm while after the encapsulation of the complex **1**, **2**, **3**, or **4**, the hydrodynamic size of the NPs increases to 144.2, 141.5, 125.8, and 137.7 nm, respectively (Figure 2A and Table 2). This trend was also observed by Lippard in the case of *cis,trans,cis*-$[PtCl_2\{O_2C(CH_2)_4CH_3\}_2(NH_3)_2]$ where the size of the particles increased with the percentage of the loaded complex.[32]

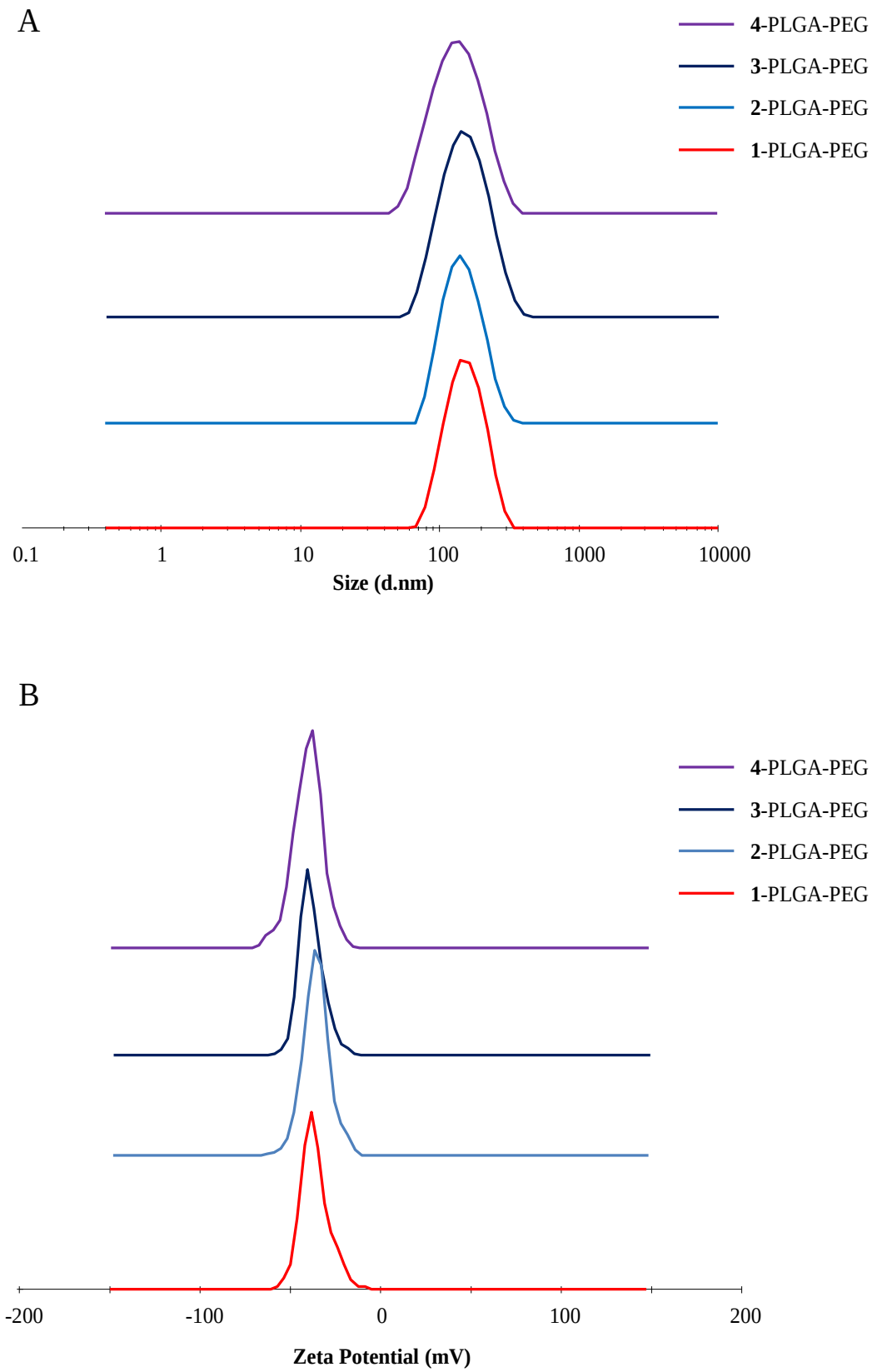

Figure 2. A) Size distribution (measured by Dynamic Light Scattering) and B) Zeta potential distribution (measured by Laser Doppler Velocimetry) of PLGA-PEG NPs loaded with **1**, **2**, **3**, or **4**.

The size distribution was described in terms of polydispersity. Light scattering can be used to describe the width of the particle size distribution. In Table 2 the term polydispersity is derived from the polydispersity index (DLS PDI), a parameter calculated from a cumulative analysis of the DLS measured intensity autocorrelation function,[56] DLS PDI values greater than 0.2 are considered to be heterogeneous, and those below 0.2 are considered to be homogeneous.[57]

The values of DLS PDI for unloaded and loaded NPs were found to be approximately 0.1 indicating a sufficiently homogenous distribution of NPs. This value is quite similar to that found for *cis,trans,cis*-$[PtCl_2\{O_2C(CH_2)_4CH_3\}_2(NH_3)_2]$ PDI = 0.171 using for encapsulation a weight of complex corresponding to 5% of the weight of loading polymer.

The surface charge of the NPs in solution (colloids) was analyzed by calculating the Zeta Potential (ZP). NPs have a surface charge that attracts a thin layer of ions of opposite charge on the nanoparticle surface. This double layer of ions travels with the nanoparticle as it diffuses throughout the solution. The electric potential at the boundary of the double layer is known as the Zeta potential of the particles and has values that typically range from +100 mV to -100 mV. The ZP is an indicator of the stability of the NP suspension. A higher electric charge on the surface of the NPs will prevent aggregation of the NPs in buffer solution because of the strong repellent forces among particles.[58,59]

As a rule of thumb, absolute ZP values above 30 mV provide good stability[60,61] and above 60 mV excellent stability. ZP distribution for PLGA-PEG NPs loaded with the four complexes is reported in Figure 2B.

The ZP values were obviously affected by the presence of PEG chains[19] and, for the unloaded PLGA-PEG nanoparticles, it resulted to be −40.0 mV, while after the encapsulation of the complexes, the absolute values decreased to −37.9 and −36.0 mV, in the case of **1** and **2**, respectively (Table 2). On the contrary, the absolute value of ZP increased with respect to unloaded NPs when the encapsulation was performed for the complexes with a smaller chain length, **3** and **4**,

(−42 and −40.2 mV, respectively, Table 2). These results confirm the good stability of the NP suspensions.

The yield, the drug encapsulation, and loading efficiency are also listed in Table 2. Drug loading (Table 2) was measured by ICP-MS and the encapsulation efficiency (EE) of the PLGA-PEG NPs was defined as the percentage of drug encapsulated, with respect to the total amount of drug used to prepare the NPs. In particular, when the encapsulation was carried out at 10% of drug feed, a consistent trend was observed. The amount of platinum complex encapsulated increased with the chain length of the carboxylate ligand (Table 2), and the most lipophilic compound (**2**) exhibited the highest encapsulation efficiency (5.8 %).

Furthermore, since logP of the carboxylic acid used as ligand correlates with the lipophilicity of the whole platinum complex,[37] the log of the encapsulation efficiency (EE) was plotted against logP of the carboxylic acid (Table 3 and Figure 3). Figure 3 shows that, as the chain length of the carboxylate ligand increases, there is a direct and predictable increase of platinum complex encapsulation. The estimated EE values are in the range of 4.2% to 5.8% for the complexes having, in the axial position, acetate and decanoate, respectively. These results indicate that lipophilic Pt(IV) derivatives of kiteplatin have a drug-loading potential towards PLGA-PEG NPs comparable to that of lipophilic Pt(IV) derivatives of cisplatin.[37] However, the log(EE%)/logP curve obtained with our derivatives (Figure 3) has a slope that is smaller than that of the analogous curve reported by Lippard for the lipophilic cisplatin Pt(IV)-derivatives.[37] This could likely be due to the presence of the more lipophilic *cis*-1,4-DACH diamine, as compared to the two ammine ligands of cisplatin, that reduces the influence of the lipophilic axial ligands on the overall lipophilicity of the complexes.

From the Pt-loading, obtained by ICP-MS, we were also able to calculate (Supporting Information) the number of Pt atoms (and hence of Pt(IV)-complex molecules) per nanoparticle (Table 2). The number of Pt atoms per nanoparticle is in the range $1.27 \cdot 10^6$-$2.36 \cdot 10^6$ and obviously reflects the Pt-loading trend. Moreover, the order of magnitude is comparable to the drug loading of

polysilsesquioxane based[62] nanoparticles that have been used for the delivery of Pt(IV)-prodrugs but considerably higher than that found for other nanoparticle platforms.[32,34,63]

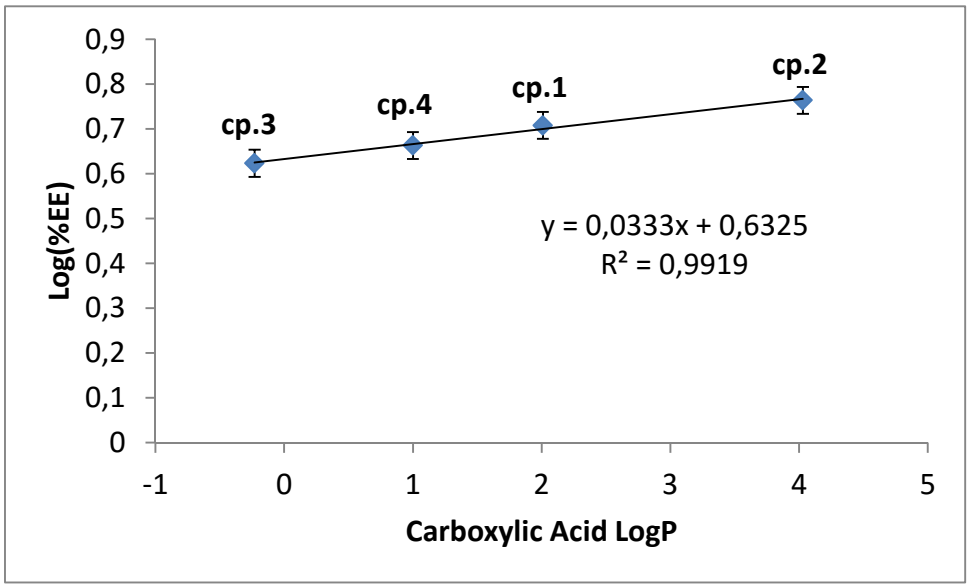

Figure 3. Correlation between the log of encapsulation efficiency (% EE) for **1** (cp. 1), **2** (cp. 2), **3** (cp. 3), and **4** (cp. 4) (ordinate) and log P of the carboxylic acids whose carboxylates constitute the axial ligands of **1**, **2**, **3**, and **4** (abscissa). See also Table 3.

The surface morphology was evaluated by TEM, and images of PLA-PEG NPs loaded with **1** and **2** are shown in Figure 4. TEM analysis showed that both drug loaded PLGA-PEG NPs do not aggregate. Furthermore, nanoparticles are characterized by a spherical shape, rather homogeneous in size: 60 ± 22 nm for **1**-PLGA-PEG NPs (Figure 4-A), 80 ± 13 nm for **2**-PLGA-PEG NPs (Figure 4-B), 58 ± 19 nm for **3**-PLGA-PEG NPs, and 55 ± 24 nm for **4**-PLGA-PEG NPs. Diameters values obtained by TEM are smaller than those detected by DLS. On the average, the measured values of the hydrodynamic diameters (mean diameters), were ca. 50% higher than the mean diameters observed by TEM; such a discrepancy is most likely due to the hydration shell of the PEG chains exposed on the surface of the nanoparticles in water suspension. Moreover, the NPs tend to shrink during the drying process performed before the TEM analysis, resulting in a size smaller than that observed in the DLS analysis.

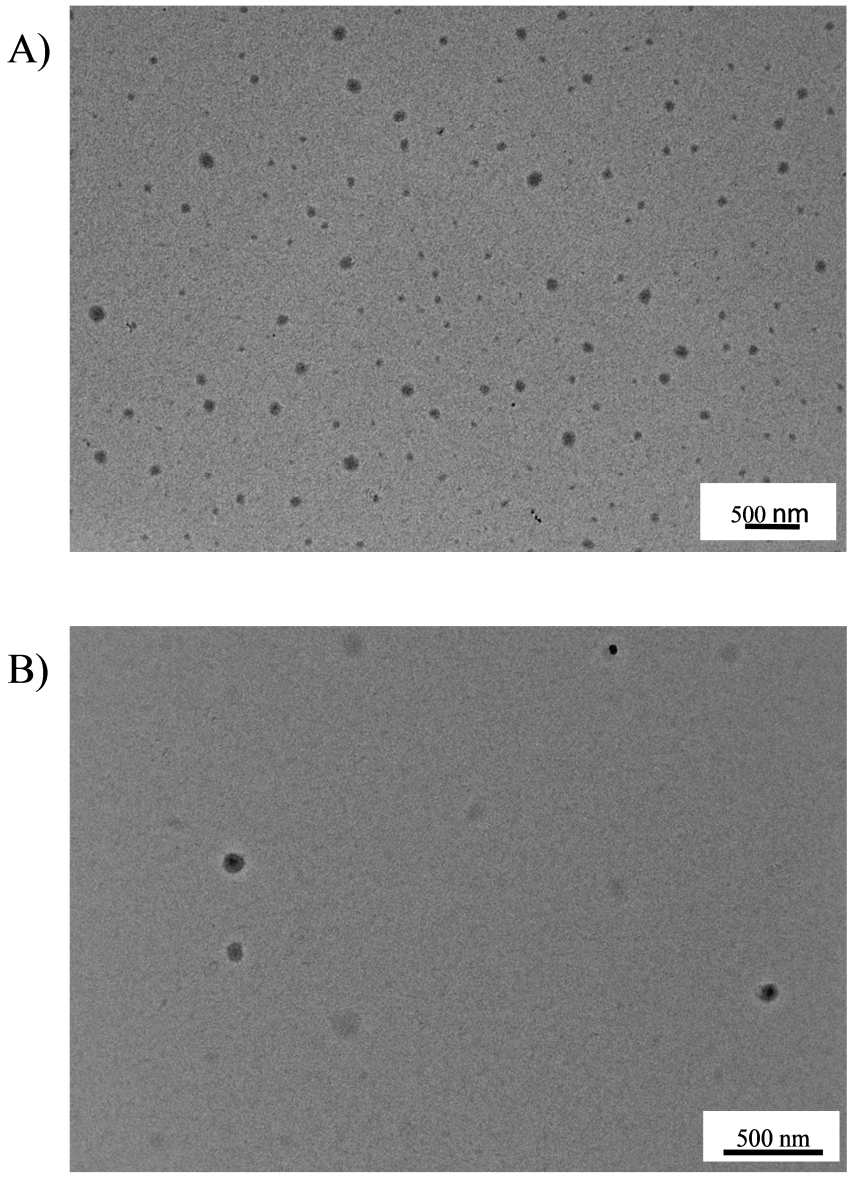

Figure 4. Transmission electron micrograph of PLGA-PEG NPs loaded with **1** (A) and **2** (B). Scale bar = 500 nm.

***In vivo* studies.**

The four complexes chosen for our investigation had already been prepared by Khokhar[38] and colleagues and two of them (**3** and **4**) were also evaluated *in vivo* in the murine L1210/0 leukemia model. The optimal dose for the two compounds (6 mg/kg/injection) was found to be similar to that of cisplatin (5 mg/kg/injection), with compound **3** having the greatest efficacy (40 % survivors). However, the *in vivo* activity of the Pt(IV) complexes with longer alkyl chains of the carboxylate ligands was not evaluated because of their poor aqueous solubility. In the present investigation, by exploiting a micellar approach, the amount of platinum complex encapsulated increased with the chain length of the carboxylate ligand, hence we selected the most lipophilic/encapsulated compounds **1** and **2** for the *in vivo* investigation.

Unloaded PLGA-PEG nanoparticles and PLGA-PEG nanoparticles loaded with **1** or **2** were evaluated for their *in vivo* antitumor activity in the Lewis lung carcinoma (LLC) syngeneic murine model resulting from the implantation of the highly tumorigenic Lewis lung carcinoma cells in C57BL mice. Being created on an immunocompetent murine background, the LLC model allows the evaluation of true immune and toxicity response with respect to targeted therapies and tumor growth. LLC is highly tumorigenic and is primarily used to model metastasis as well as evaluate the efficacy of chemotherapeutic agents *in vivo*.[64] Tumor growth inhibitions induced by unloaded and **1** or **2** loaded nanoparticles were compared with those promoted by the two reference platinum agents, kiteplatin and CDDP. Seven days after tumor inoculation, tumor-bearing mice were randomized into vehicle control and treatment groups (5 mice per group). Control mice received the vehicle (saline solution), whereas treated groups received daily doses of unloaded PLGA-PEG nanoparticles, **1** or **2** (1.7 $mg \cdot kg^{-1}$) loaded on PLGA-PEG nanoparticles, kiteplatin or cisplatin (1.7 $mg \cdot kg^{-1}$ in saline solution). Tumor growth was estimated at day 15, and the results are reported in Table 4. As an indication of the adverse side effects, changes in the body weights of tumor-bearing mice were monitored every two days (Figure 5). The administration of unloaded PLGA-PEG nanoparticles did not result in inhibition of tumor growth. On the contrary, PLGA-PEG

nanoparticles loaded with **1** or **2** induced a 77.8% and 81.9% tumor regression, respectively. Kiteplatin and cisplatin, at the same daily dose, induced a tumor mass reduction of 73.7% and 81.7%, respectively. Thus, the data indicate Pt(IV) prodrugs derived from kiteplatin (**1** and **2**) loaded on PLGA-PEG nanoparticles are significantly more effective than kiteplatin itself in inhibiting tumor growth and **2** is slightly more effective than **1**. This result increases in significance if we consider that, having administered equal weights of the three drugs (1.7 mg/Kg), in terms of administered moles **2** is less than **1** and **1** is less than kiteplatin (0.51:0.61:1). Cisplatin is as effective as **2** loaded on PLGA-PEG nanoparticles in inhibiting tumor growth but, again, we have to consider that in terms of moles **2** is given in smaller amount than cisplatin (0.41:1).

The different amount of moles of platinum administered in the different cases is reflected on the changes in body weights (Figure 5) with cisplatin inducing clear signs of anorexia, kiteplatin being slightly better (roughly 16% decrease of mice body weight), and PLGA-PEG nanoparticles loaded with **1** or **2** being much better (body weight loss <5%). Thus, in the case of **2** loaded on PLGA-PEG we combine the highest response to platinum targeted therapy with the smallest toxicity.

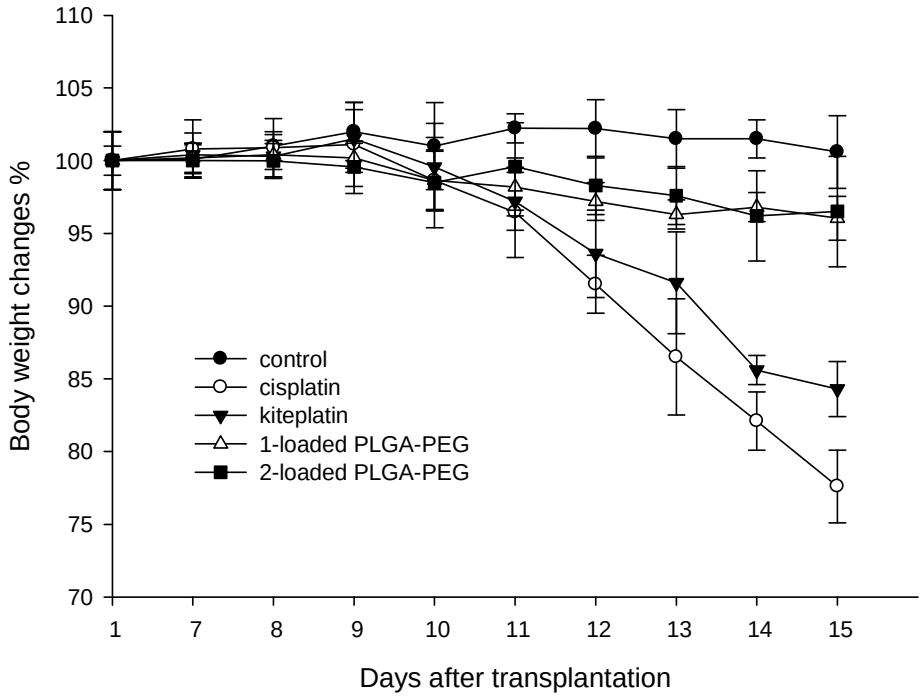

Figure 5. Body weight changes of LLC bearing C57BL mice treated with vehicle or tested compounds. Each compound was administered daily after 7 days from the tumor cell inoculum. Weights were measured at day 1 and daily from day 7. Error bars indicate the standard deviation.

Conclusions

In this work we have synthesized four Pt(IV) prodrugs of kiteplatin, complexes **1**, **2**, **3** and **4**, having in the axial positions four different carboxylato ligands (hexanoate, decanoate, acetate and butanoate, respectively). The high lipophilicity of these ligands have been exploited for encapsulation of the corresponding Pt(IV) prodrugs in the hydrophobic core of PLGA-PEG NP (kiteplatin itself is too hydrophilic to be entrapped into the hydrophobic core of this kind of micelles). The stability of the NPs suspensions (obtained by nanoprecipitation methods) was good as evidenced by their measured zeta potential while TEM analysis showed that PLGA-PEG NPs loaded with **1** or **2** are characterized by a spherical shape and rather homogeneous size. The drug

encapsulation efficiency (EE) was found to be correlated to the different lipophilicity of the four Pt(IV) prodrugs. In particular, it was found that, as the chain length of the axial carboxylato ligands increases, also the degree of encapsulation of the Pt(IV) complexes increases with *ca.* two million drug molecules loaded per nanoparticle.

The idea behind this work was that, after degradation of the NPs, the reduction of the Pt(IV) prodrug to the corresponding Pt(II) species in the tumor cell would afford the cytotoxic kiteplatin payload, possibly with reduced systemic toxicity. The *in vivo* experiments carried out with NPs loaded with **1** or **2** (these complexes are characterized by the highest encapsulation efficiency), confirmed that the nanodrugs possess an higher antitumor effect with respect to kiteplatin but, most importantly, they show a marked reduced toxicity. This latter issue is one of the most important targets in the current research for alternative drugs and/or delivery systems to clinically used platinum drugs.

Acknowledgments.

We acknowledge the University of Bari (Italy), the Italian Ministero dell'Università e della Ricerca (FIRB RINAME RBAP114AMK and PON02_00607_3621894), the Inter-University Consortium for Research on the Chemistry of Metal Ions in Biological Systems (C.I.R.C.M.S.B.), and the European Union (COST CM1105: Functional metal complexes that bind to biomolecules) for support.

Supporting Information

NMR characterization of **1** (^{1}H NMR, COSY, [^{1}H-^{195}Pt]-HSQC, and [^{1}H-^{13}C] HSQC), **2** (^{1}H NMR, TOCSY, [^{1}H-^{195}Pt]-HSQC, and [^{1}H-^{13}C] HSQC), and PLGA-PEG (FT-IR spectrum); calculation of Pt atoms per NP.

Table of Content graphic

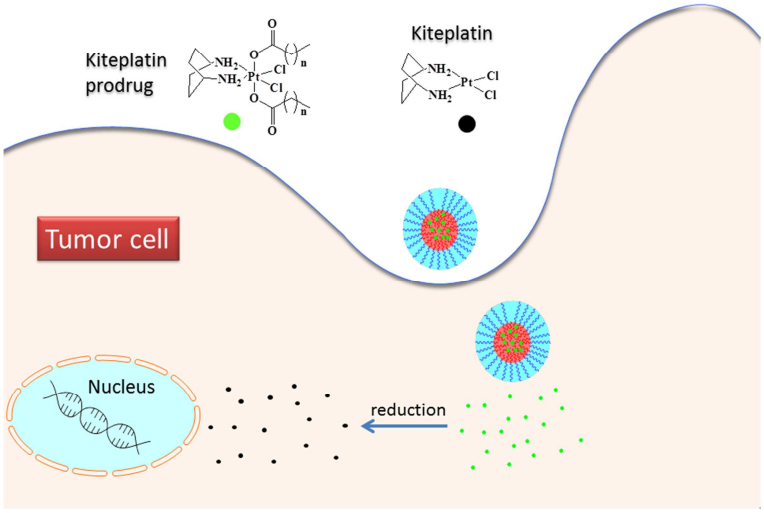

PLGA-PEG nanoparticles loaded with Pt(IV) prodrugs of kiteplatin boost the antitumor effect of the drug and reduce its toxicity.

Table 1. Average Molecular Weights and Polydispersity of PLGA-PEG copolymer.

$\mathbf{M_n}$[a] kDa ± SD	$\mathbf{M_w}$[b] kDa ± SD	$\mathbf{M_p}$[c] kDa ± SD	**SEC PDI**[d] (M_w/M_n)
25.5 ± 2.2	25.8 ± 1.0	26.0 ± 1.3	1.003 ± 0.002

[a]Number average molecular weight (M_n); [b]Weight average molecular weight (M_w); [c] Molar mass at the peak maximum (M_p); [d] Polydispersity index (SEC PDI).

Table 2. Physicochemical characteristics of PLGA-PEG NPs.

NPs	Size[a] (nm)	DLS PDI[b]	ZP[c] (mV)	DL%[d]	EE%[e]	Pt_{atoms}/NP[f]
Unloaded PLGA-PEG	116.6 ± 1.4	0.124 ± 0.001	-40.0 ± 0.9	-	-	-
1-PLGA-PEG	144.2 ± 0.9	0.103 ± 0.034	-37.9 ± 0.3	0.161	5.1±1.3	$1.91 \cdot 10^6$
2-PLGA-PEG	141.5 ± 2.3	0.110 ± 0.007	-36.0 ± 2.0	0.142	5.8±1.6	$2.36 \cdot 10^6$
3-PLGA-PEG	125.8 ± 0.2	0.105 ± 0.032	-42.0 ± 1.6	0.164	4.2±1.3	$1.27 \cdot 10^6$
4-PLGA-PEG	137.7 ± 0.1	0.127 ± 0.020	-40.2 ± 1.3	0.157	4.6±1.2	$1.61 \cdot 10^6$

[a]Average hydrodynamic diameter; [b]DLS PDI = polydispersity index; [c]ZP = zeta potenzial; [d]DL% = Drug Loading (% Pt in loaded nanoparticles); [e]EE% = encapsulation efficiency (data are shown as media ± SD; n=3); [f]Pt_{atoms}/NP = number of Pt atoms contained in a single nanoparticle (Supporting Information).

Table 3. Log(EE%) values for complexes **1**, **2**, **3**, and **4** and logP values for corresponding carboxylic acid.

Complexes	Carboxylic acid	Carboxylic Acid LogP	Log(%EE)
1	Hexanoic acid	2.01	0.71
2	Decanoic acid	4.03	0.76
3	Acetic acid	-0.23	0.62
4	Butanoic acid	1	0.66

Table 4. *In vivo* antitumor activity.

	Daily dose *i.p.* (mg kg^{-1})	Average tumor weight (mean ± SD, g)	Inhibition of tumor growth (%)
Control[a]	-	0.563±0.14	-
Unloaded PLGA-PEG	-	0.560±0.09	0.5
1-loaded PLGA-PEG	1.7	0.125±0.05	77.8
2-loaded PLGA-PEG	1.7	0.102±0.04	81.9
kiteplatin	1.7	0.148±0.08	73.7
cisplatin	1.7	0.103±0.07	81.7

[a] vehicle (saline solution). Starting from day 7 after tumor implantation, tested compounds were daily administered intraperitoneally (*i.p.*). At day 15, mice were sacrificed, and tumor growth was detected as described in the Experimental Section. All reported values are the means ± SD of no less than three measurements.

References

[1] N. J. Wheate, S. Walker, G. E. Craig, R. Oun. *Dalton Trans*. 2010, **39**, 8113−8127.

[2] L. Kelland. *Nat. Rev. Cancer*. 2007, **7**, 573−584.

[3] O. C. Farokhzad, R. Langer. *ACS Nano*. 2009, **3**, 16−20.

[4] T.M. Allen, P.R. Cullis. *Science*. 2004, **303**,1818–1822.

[5] D.A. LaVan, T. McGuire, R. Langer. *Nat. Biotechnol*. 2003, **21**, 1184–1191.

[6] I. Brigger, C. Dubernet, P. Couvreur. *Adv. Drug Deliv. Rev*. 2002, **54**, 631–651.

[7] L. Brannon-Peppas, J.O. Blanchette. *Adv. Drug Deliv. Rev*. 2004, **56**, 1649–1659.

[8] T.M. Fahmy, P.M. Fong, A. Goyal, W.M. Saltzman. *Mater. Today*. 2005, **8**, 18–26.

[9] T. C. Johnstone, K. Suntharalingam, S. J. Lippard. *Chem. Rev*. 2016, **116**, 3436−3486.

[10] X. Wang, Z. Guo. *Chem. Soc. Rev.* 2013, **42**, 202-234.

[11] E. Gabano, M. Ravera, D. Osella. *Curr. Med. Chem*. 2009, **16**, 4544-4580.

[12] H.S. Oberoi, N.V. Nukolova, A.V. Kabanov, T.K. Bronich. *Adv. Drug Deliv. Rev.* 2013, **65**, 1667-1685.

[13] L. Messori, A. Merlino. *Coord. Chem. Rev.* 2016, **315**, 67-89.

[14] S.M. Moghimi, S.S. Davis. *Crit. Rev. Ther. Drug*. 1994, **11**, 31–59.

[15] G. Storm, S.O. Belliot, T. Daemen, D.D. Lasic *Adv. Drug. Deliv. Rev*. 1995, **17**, 31–48.

[16] D.C. Litzinger, A.M.J. Buiting, N. Vanrooijen, L. Huang. *BBA-Biomembranes* 1994, **1190**, 99–107.

[17] S. Stolnik, C.R. Heald, J. Neal, M.C. Garnett, S.S. Davis, L. Illum, S.C. Purkis, R.J. Barlow, P.R. Gellert. *J. Drug Target*. 2001, **9**, 361–378.

[18] S. Stolnik, L. Illum, S.S. Davis. *Adv. Drug Del. Rev*. 1995, **16**, 195–214.

[19] Y.P. Li, Y.Y. Pei, X.Y. Zhang, Z.H. Gu, Z.H. Zhou, W.F. Yuan, J.J. Zhou, J.H. Zhu, X.J. Gao. *J. Control. Rel.*, 2001, **71**, 203–211.

[20] R. Gref, Y. Minamitake, M.T. Perracchia, V. Trubetskoy, V. Torchilin, R. Langer *Science*, 1994, **263**, 1600–1603.

[21] M. Tobío, R. Gref, A. Sánchez, R. Langer, M.J. Alonso. *Pharm. Res.* 1998, **15**, 270–275.

[22] P. Quellec, R. Gref, L. Perrin, E. Dellacherie, F. Sommer, J.M. Verbavatz, M.J. Alonso. *J. Biomed. Mater. Res.* 1998, **42**, 45–54.

[23] M.T. Peracchia, C. Vauthier, C. Passirani, P. Couvreur, D. Labarre. *Life Sci*. 1997, **61**, 749–761.

[24] S. Stolnik, S.E. Dunn, M.C. Garnett, M.C. Davies, A.G.A.Coombes, D.C. Taylor, M.P. Irving, S.C. Purkiss, T.F. Tadros, S. Davis. *Pharm. Res*. 1994, **11**, 1800–1808.

[25] D. Bazile, C. Prud'homme, M.T. Bassoullet, M. Marlard, G. Spenlehauer, M. Veillard *J. Pharm. Sci.* 1995, 84, 493–498.

[26] M.T. Peracchia, R. Gref, Y. Minamitake, A. Domb, N. Lotan, R. Langer. *J. Control. Release*. 1997, 46, 223–231.

[27] B. Jeong, Y.H. Bae, S.W. Kim. *J. Control. Release* 2000, **63**, 155–163.

[28] O.C. Farokhzad, S. Jon, A. Khademhosseini, T-N.T. Tran, D.A. LaVan, R. Langer. *Cancer Res*. 2004, **64**, 7668–7672.

[29] S.E. Lupold, B.J. Hicke, Y. Lin, D.S. Coffey. *Cancer. Res*. 2002, **62**, 4029–4033.

[30] R.S. Israeli, C.T. Powell, W.R. Fair, W.D.W. Heston. *Cancer Res*. 1993, **53**, 227–230.

[31] G.P. Murphy, A.A. Elgamal, S.L. Su, D.G. Bostwick, E.H. Holmes. *Cancer*. 1998, **83**, 2259–2269.

[32] S. Dhar, F.X. Gu, R. Langer, O.C. Farokhzad, S.J. Lippard. *PNAS*, 2008, **105**, 17356-17361.

[33] K.R. Barnes, A. Kutikov, S.J. Lippard. *Chem. Biol*., 2004, **11**, 557–564.

[34] R.P. Feazell, N. Nakayama-Ratchford, H. Dai, S.J. Lippard. *J. Am. Chem. Soc*. 2007, **129**, 8438–8439.

[35] S. Dhar, Z. Liu, J. Thomale, H. Dai, S. J. Lippard. *J. Am. Chem. Soc*. 2008, **130**, 11467-11476.

[36] S. Mukhopadhyay, C. M. Barnés, A. Haskel, S. M. Short, K. R. Barnes, S. J. Lippard. *Bioconjugate Chem*., 2008, **19**, 39-49.

[37] T.C. Johnstone, S.J. Lippard. *Inorg. Chem.*, 2013, **52**, 9915–9920.

[38] S. Shamsuddin, C. C. Santillan, J. L. Stark, K. H. Whitmire, Z. H. Siddik, A. R. Khokhar. *J. Inorg. Biochem.* 1998, **71**, 29-35.

[39] N. Margiotta, C. Marzano, V. Gandin, D. Osella, M. Ravera, E. Gabano, J.A. Platts, E. Petruzzella, J.D. Hoeschele, G. Natile. *J. Med. Chem.* 2012, **55**, 7182-7192.

[40] R. Ranaldo, N. Margiotta, F. P. Intini, C. Pacifico, G. Natile. *Inorg. Chem*. 2008, **47**, 2820-2830.

[41] J. Kasparkova, T. Suchankova, A. Halamikova, L. Zerzankova, O. Vrana, N. Margiotta, G. Natile, V. Brabec. *Biochem. Pharmacol.* 2010, **79**, 552-564.

[42] V. Brabec, J. Malina, N. Margiotta, G. Natile, J. Kasparkova, *Chem. Eur. J.* 2012, **18**, 15439-15448.

[43] N. Margiotta, E. Petruzzella, J. A. Platts, S. T. Mutter, R. J. Deeth, R. Ranaldo, P. Papadia, P. A. Marzilli, L. G. Marzilli, J. D. Hoeschele, G. Natile. *Dalton Trans*., 2015, **44**, 3544-3556.

[44] S. T. Mutter, N. Margiotta, P. Papadia, J. A. Platts. *J. Biol. Inorg. Chem*. 2015, **20**, 35-48.

[45] E. Petruzzella, N. Margiotta, G. Natile, J. D. Hoeschele, *Dalton Trans.*, 2014, **43**, 12851-12859.

[46] E. Petruzzella, N. Margiotta, M. Ravera, G. Natile. *Inorg. Chem*. 2013, **52**, 2393−2403.

[47] P. S. Pregosin. *Coord. Chem. Rev.* 1982, 44, 247-291.

[48] J. Cheng, B.A Teply, I. Sherifi, J. Sung, G. Luther, F.X. Gu., E. Levy Nissenbaun, A.F. Radovic Moreno, R. Langer, O.C. Farokhzed. *Biomaterials*, 2007, **28**, 869–876.

[49] M. R. Reithofer, M. Galanski, A. Roller, B. K. Keppler. *Eur. J. Inorg. Chem.* 2006, 2612-2617.

[50] M. R. Reithofer, S. M. Valiahdi, M. A. Jakupec, V. B. Arion, A. Egger, M. Galanski, B. K. Keppler. *J. Med. Chem.* 2007, **50**, 6692-6699.

[51] K. R. Barnes, A. Kutikov, S. J. Lippard. *Chem. & Bio.*, 2004, **11**, 557-564.

[52] M.P. Stevens. *Polymer Chemistry: An Introduction, Oxford University Press; 3rd International edition*, **2009.**

[53] F. von Burkersroda, R. Gref, A. Göpferich, *Biomaterials*, 1997, **18**, 1599–1607.

[54] S. Essa, J.M. Rabanel, P. Hildgen, *Eur. J. Pharm. Biopharm*. 2010, *75*, 96-106

[55] N. Kolishetti, S. Dhar, P.M. Valencia, L.Q. Lin, R. Karnik, S.J. Lippard, R. Langer, O.C. Farokhzad. *PNAS*, 2010, **107**, 17939-17944.

[56] D.E. Koppel. *The Journal of Chemical Physics*. 1972, **57**, 4814-4820.

[57] R.N. Johnson, P. Kopečková, J. Kopeček. *Bioconjug. Chem*., 2009, **20**, 129–137.

[58] K. Sawant, S. Dodiya. *Recent Pat. Drug Deliv. Formul.* 2008, **2**, 120-135.

[59] U. Kedar, P. Phutane, S. Shidhaye, V. Kadam *J. Nanomed. Nanotechnol*. 2010, **6**, 714–729.

[60] S.A. Wissinga, O. Kayserb, R.H. Muller. *Adv. Drug Deliver. Rev.* 2004, **56**, 1257– 1272.

[61] C. Jacobs, O. Kayser, R.H. Muller. *Int. J. Pharm*. 2000, **196**, 161–164.

[62] J. Della Rocca, R.C. Huxford, E. Comstock-Duggan, W. Lin. *Angew. Chem. Int. Ed.* 2011, **50**, 10330-10334.

[63] Y. Min, C. Mao, D. Xu, Y. Liu. *Chem. Commun.* 2010, **46**, 8424-8426.

[64] Y. Sakai, T. Sasahira, H. Ohmori, K. Yoshida, H. Kuniyasu. *Virchows Arch*. 2006, **449**, 341–347.